

# Lattice Dynamics of Carbon Chain Inside a Carbon Nanotube

Z. X. Guo,<sup>†</sup> J. W. Ding,<sup>\*,†,‡</sup> Y. Xiao,<sup>†</sup> and Y. L. Mao<sup>†</sup>

Department of Physics, Xiangtan University, Xiangtan 411105, Hunan, China, and National Laboratory of Solid State Microstructures, Nanjing University, Nanjing 210093, China

Received: June 14, 2006; In Final Form: August 22, 2006

Based on the density functional theory, we obtain the optimum geometry of carbon chain inside a carbon nanotube. The phonon spectrum and specific heat of such a chain and nanotube hybrid system are calculated in terms of lattice dynamics theory. Some new phonon branches that have been obtained come from the coupling vibrations of the nanotube and the chain. The bending and stretching modes of the chain appear at about 520  $\text{cm}^{-1}$  and 1935  $\text{cm}^{-1}$  at  $\Gamma$  point, respectively. It is found that the softening of G modes results mainly from the chain induced variations in the bond length on nanotube, independent of van der Waals interaction, while the stiffening of radial breathing mode is developed by the competition between the two factors. In the low-frequency region, the vibrational density of states are very different from that of the bare nanotube. Its specific heat implies the underlying quantized phonon structures and much large thermal conductivity in the hybrid system. In addition, the chain-length dependent vibration modes are calculated, from which it is expected that a finite chain of about 14 carbon atoms in the nanotube may produce the experimental Raman peak at about 1850  $\text{cm}^{-1}$ .

## Introduction

Single-walled carbon nanotubes (SWCNs) have attracted much attention due to their unique electronic and mechanical properties, such as controllable band structure, high mechanical strength, high thermal and chemical stability, and excellent heat conduction,<sup>1–5</sup> which have been considered as a promising class of quasi-one-dimensional nanostructures meeting several requirements and offering new paradigms in nanodevices.<sup>6,7</sup> Especially, the hollow cylindrical structure of the nanotube is an ideal container for some atoms or small molecules. Capillary action of atoms and molecules into the tubes has been theoretically and experimentally studied.<sup>8–12</sup> Because of confinement inside the tube, the encapsulated atoms or molecules may form some new phases. It is shown<sup>9,10,13,14</sup> that the electronic properties of the doped tubes are not a simple sum of those of the constituent units. The combined materials may be insulators, metals, and superconductors under certain conditions.

Recently, a new combined system, carbon nanowire (CNW), is formed by a carbon atom chain doped into the core of the SWCN, which had been observed by high-resolution transmission electron microscope.<sup>15,16</sup> It is shown that such a CNW has high thermal and mechanical stability due to the van der Waals forces.<sup>15</sup> For their unique physical properties of both carbon chain and SWCN, it is very interesting to explore the possible new phenomena within this new combined system, such as specific heat and thermal transport. From a practical point of view, good thermal managements of CNWs have potential applications of future nanotube-based thermoelectrical devices, which can greatly improve the performance of the nanosized devices due to heat dissipations.

For the applications of the CNW-based devices, one needs to characterize the geometry of CNWs. The resonant Raman-scattering technique has been shown to provide a powerful tool for studying and characterizing the SWCNs, for which the radial breathing mode (RBM) and the tangential mode vibrations (so-called G modes) are the two main features in the Raman spectra. Recently, the unusual Raman spectral features at both low and high frequencies were observed in the CNWs, which was ascribed to the vibration of the chain in the nanotube.<sup>16–18</sup> This means that the lattice dynamics study of the CNWs may be of particular importance in the characterization and thermal managements in the CNW-based molecular devices.

The carbon chains in the CNW may not be continuous, comprising some shorter segments, in which the C–C distances  $d_{\text{cc}}$  differ from those in free short carbon chains. Experimentally, the Raman peak was observed at about 1850  $\text{cm}^{-1}$ , which was ascribed to the finite length of the carbon chain.<sup>19,20</sup> Therefore, it would be interesting to study the chain-length dependent vibration modes, which may provide a probe to identify the various lengths of chains confined in a nanotube.

In this paper, we first optimize the geometry of CNW, based on density functional theory. The phonon spectrum and specific heat are calculated in terms of lattice dynamics theory. Some new phonon branches have been obtained, come from the coupling vibrations of the nanotube and the chain. The bending and stretching modes of the chain appear at about 520  $\text{cm}^{-1}$  and 1935  $\text{cm}^{-1}$ , respectively. The softening of G modes is observed due to the chain induced variations in the bond length on nanotube, independent of van der Waals interaction, while the stiffening of RBM is developed by the competition between the two factors. The results are at variance with the isolated carbon nanotube. In the low-frequency region, the vibrational density of states (DOS) are very different from that of the bare nanotube. The calculated specific heat implies the underlying quantized phonon structures and much large thermal conductivity in such quasi-one-dimensional hybrid system. In addition,

\* Corresponding author phone: 86-732-829329; fax: 86-732-8292468; e-mail: jwding@xtu.edu.cn.

<sup>†</sup> Xiangtan University.

<sup>‡</sup> Nanjing University.

the chain-length dependent vibration modes are calculated, from which it may be expected that a finite chain of about 14 carbon atoms in the nanotube may produce the experimental Raman peak at about  $1850\text{ cm}^{-1}$ .

## II. Geometry Optimizations

As a typical example, we consider an CNW with a (5,5) tube outside (defined by (5,5) CNW). This is because its tube radius of about  $3.4\text{ Å}$  is closest to that of the innermost tube observed experimentally.<sup>15,16</sup> To achieve the most stable structure of the (5,5) CNW, the first-principle calculations based on density functional theory have been performed using the CASTEP code.<sup>21</sup> GGA (generalized gradient approximation) exchange-correlation functional<sup>22</sup> and ultrasoft pseudopotentials were employed.<sup>23</sup> The cutoff energy is 350 eV for a plane-wave basis set. Optimal atomic positions are determined until the magnitude of the forces acting on all atoms became less than  $0.03\text{ eV/Å}$ , which also converged the total energy within  $0.01\text{ meV}$ . The CNW was modeled by a periodically repeating unit cell. With the CNW lying along the  $c$  direction, the lattice parameters  $a$  and  $b$  were chosen to ensure a minimum distance of more than  $10\text{ Å}$  between two nearest neighboring outer-walls, so that the interactions between an CNW and its periodic images were negligible.

To simplify the calculations, the value of  $c$  was set to be the length of the translation vector of the tube along the axial direction. We optimize the structures of the CNW with two inserted carbon atoms in a supercell. The initial C–C distance in the chain corresponds to the minimum points of the total energy with respect to  $d_{cc}$ , as reported by one of the authors.<sup>24</sup> For the relaxed structure, the C–C distance  $d_{cc}$  in the chain, tube diameter  $D$ , and unit cell length  $L$  of the nanotube are 1.229, 6.801, and 2.458 in units of Å, respectively, which are in good agreement with previous results.<sup>16,24,25</sup> Compared with the bare (5,5) tube of  $D = 6.795\text{ Å}$  and  $L = 2.440\text{ Å}$ , the tube geometry in the CNW is slightly altered by the inserted carbon chain. The energy dispersion is also calculated, and no energy gap is observed at about Fermi energy, consistent with the result by Mao et al.<sup>24</sup>

To confirm the result obtained above, we have further considered a larger supercell, containing three nanotube unit cells but various carbon atom number  $n$  ( $n = 5, 6, 7$ ) in the core chain. The total atom number of the supercell is 65, 66, and 67 at  $n = 5, 6$ , and  $7$ , respectively. The corresponding  $d_{cc}$  in the chains is of about 1.47, 1.23, and  $1.05\text{ Å}$ . The most stable structure is found to be a commensurate one with the same C–C bond length of  $1.229\text{ Å}$ , corresponding to that of  $n = 6$  in the supercell, while some incommensurate structures are usually expected for different carbon system. The result is consistent with that obtained by Ruzsnyák et al. using the local density approximation (LDA) performed with the VASP code.<sup>25</sup> Therefore, the structure of the CNW with one nanotube unit cell may be reasonably applied in the study of the lattice dynamics of an CNW.

## III. Force Constant Model

To study the lattice dynamics of an CNW, the vibration of the outside tube can be modeled using a set of force constants of graphene up to the fourth next neighboring interaction.<sup>2</sup> The curvature effects on the C–C force constants have been corrected through a simple equation:<sup>26</sup>

$$K_{cc} = AK_g + 6AU(r_g - r_{cc})/b^3 \quad (1)$$

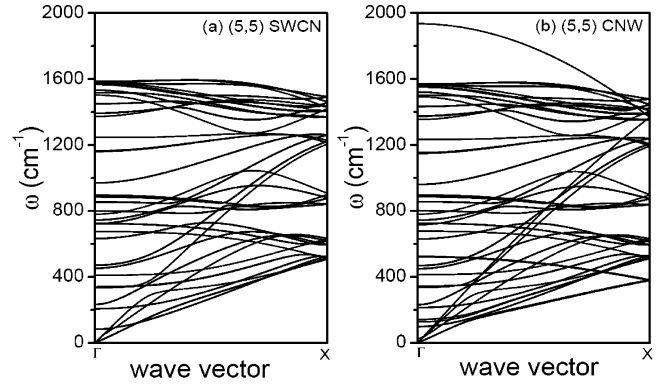


**Figure 1.** Phonon dispersion relation of the (5,5) SWCN (a) and (5,5) CNW (b).

with  $A = (6.43 + 4.17\cos\Phi)/10.6$ , where  $\Phi$  is the angle between two neighboring  $\pi$  orbitals of carbon atoms.  $K_{cc}$  ( $r_{cc}$ ) and  $K_g$  ( $r_g$ ) are the bond-stretching force constants (the equilibrium distances) of the nanotube and the graphene, respectively.  $U$  is the cohesion energy per bond and  $b$  is the Morse potential parameter achieved from the graphene bond-stretching force constants. Such corrections had been used to reproduce well the Raman mode, especially the RBM observed by experiments.

For the parameter  $A$  in the CNW, it may be simply taken to be the same with that of the bare (5,5) tube. This can be understood by the fact that the slight variation in the tube geometry has a little influence on the phonon spectrum of the CNW. As a result,  $K_{cc}$  is mainly determined by the C–C bond distance  $r_{cc}$  on the nanotube, obtained from the optimized structure above. In our calculation, we take  $U = 3.7\text{ eV}$ , and the constant  $b$  is chosen to obtain the correct bond-stretching force constant. The first and second nearest neighboring bond-stretching force constants are given by  $K_g^1 = 22.78\text{ eVÅ}^2$  and  $K_g^2 = 5.49\text{ eVÅ}^2$ , respectively.<sup>26</sup> For example, the nearest neighboring bond-stretching force constants of the nanotube are obtained to be  $K_{cc}^1 = 22.90, 22.59, \text{ and } 22.12\text{ eVÅ}^2$  at  $r_{cc} = 1.413, 1.416, \text{ and } 1.420\text{ Å}$ , respectively.

To simulate the interaction between the carbon atoms in the chain, we consider the Tersoff–Brenner bond order potential with the parameters in potential  $I$ .<sup>27</sup> Here, the conjugate compensation term  $F$  in the original function is neglected, as did in refs 28 and 29.

As for the van der Waals interaction between the chain and the nanotube, it is described by the Lennard-Jones potential:

$$u(r) = 4\epsilon \left[ -\left(\frac{\delta}{r}\right)^6 + \left(\frac{\delta}{r}\right)^{12} \right] \quad (2)$$

with the parameters  $\epsilon = 2.41\text{ meV}$  and  $\delta = 3.4\text{ Å}$ .

## IV. Calculations and Discussion

**A. Phonon Dispersion and Raman Modes.** In Figure 1 we show the phonon dispersions of both the (5,5) CNW and bare (5,5) SWCN. There are three acoustic modes in the CNW: two transverse (TAs), one longitudinal (LA), as in the bare SWCN. Twisting mode (TW) of the (5,5) CNW has a nonzero frequency of about  $27\text{ cm}^{-1}$ , higher than  $9\text{ cm}^{-1}$  of the lowest optical phonon mode, which is caused by the coupling vibrations of the chain and tube parallel to the tube axis. Also, there occur the coupling vibrations of the chain and tube vertical to the tube axis, forming two optical phonons of about  $129\text{ cm}^{-1}$  and  $143\text{ cm}^{-1}$  at  $\Gamma$  point. For the carbon chain in the CNW, there appear two bending modes at about  $520\text{ cm}^{-1}$ , and one stretching mode at about  $1935\text{ cm}^{-1}$  in the Brillouin zone center. Recent

**TABLE 1: Frequencies of RBM and G Modes for the (5,5) CNW and (5,5) SWCN (in units of  $\text{cm}^{-1}$ )**

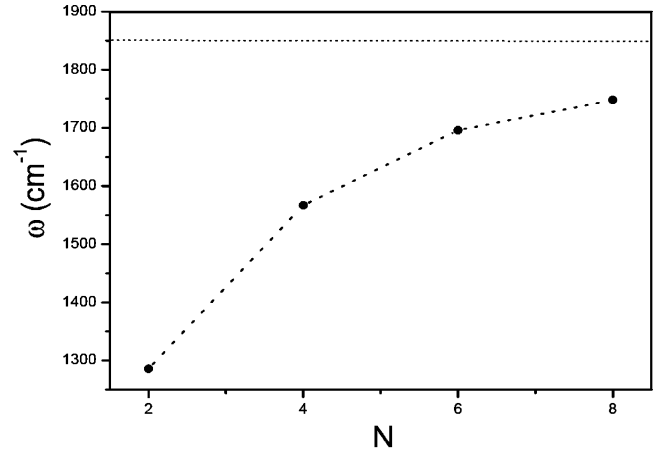
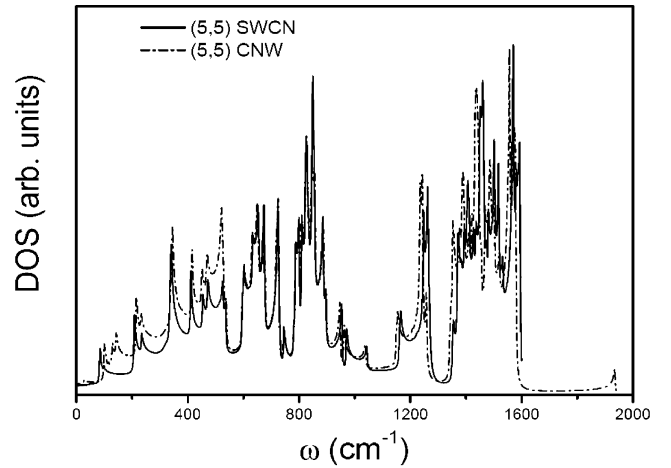
	RBM	G modes		
		$E_{2g}$	$A_{1g}$	$E_{1g}$
SWCN	335	1582	1576	1567
CNW	337	1571	1566	1550

Raman scattering experiments had identified a strong peak around  $1850 \text{ cm}^{-1}$  in a multiwall carbon nanotube containing carbon chains.<sup>16</sup> For the stretching mode, the frequency in experiment is lower than the calculated result, maybe since the measured chains comprise the shorter segments separated by vacancies.<sup>19,20</sup> This suggests a possible origin of the peak in the Raman spectrum.

Table 1 present the calculated RBM and G modes of the (5,5) SWCN and (5,5) CNW, respectively, located at low- and high-energy regions. Due to the inserted carbon chain, obviously, the G mode frequencies in the CNW are less than those in the SWCN, downshifted by about  $10\text{--}17 \text{ cm}^{-1}$ , while the RBM frequency has a little upshift of about  $2 \text{ cm}^{-1}$ , higher than  $335 \text{ cm}^{-1}$  of the bare SWCN. This provides a simple way to distinguish the CNWs from the nanotubes by the Raman spectroscopy. To investigate the origin of such Raman frequency shiftment, we recalculated the frequencies of the RBM and G modes in the CNW by neglecting the van der Waals interaction. As a result, nearly no change is observed in the G modes, indicating their independence of van der Waals interaction. From the first principle calculations, on the other hand, the C–C bond length on the nanotube is slightly increased due to the carbon chain insertion. This may lead to the decrease of force constants and thus the downshift of the G modes in the CNW. For the RBM, its frequency is downshifted to be about  $332 \text{ cm}^{-1}$ , lower than  $335 \text{ cm}^{-1}$  of the bare SWCN. This is also due to the chain induced variations in bond length on nanotube, just as the G modes in the absence of the van der Waals interaction. In the presence of the van der Waals interaction; however, the RBM would upshift from  $332$  to  $337 \text{ cm}^{-1}$ , increased by about  $5 \text{ cm}^{-1}$ . Therefore, it is the competition between the two factors of the van der Waals interaction and the chain induced variations in the bond length on nanotube that leads to the frequency shiftment in RBM.

To further probe the dependence of vibration modes on the carbon chain length, the finite length chains with  $N$  carbon atoms are considered to be confined in the core of a nanotube. Two carbon chain segments in the neighboring supercells of the CNW are separated large enough so that the interaction between two segments may be neglected. The most stable geometry structures and the phonon dispersions are then calculated for the chains of  $N=2, 4, 6$ , and  $8$ . Figure 2 shows the calculated frequencies of the stretching modes as a function of  $N$ . From Figure 2, it is found that the frequency increases with  $N$  increasing, tending to the experimental Raman peak of  $1850 \text{ cm}^{-1}$ , indicated by the dotted line. Interestingly, it may be expected that a finite chain of about 14 carbon atoms in the nanotube may produce the experimental Raman peak. The similar result was also predicated by Liu et al.,<sup>20</sup> while the length of finite chain is larger than that predicted by Fantini et al.<sup>19</sup> in another different carbon chain system. This indicates that the vibration modes are very sensitive to the chain length, which would provide a way to identify the various lengths of chains confined in nanotube.

**B. Vibrational Density of States and Specific Heat.** To explore the thermal properties of the CNWs, we first calculated in Figure 3 the DOS of (5,5) CNW and (5,5) SWCN. Compared

**Figure 2.** The calculated frequencies of the stretching modes as a function of the atom number  $N$  in the carbon chain.**Figure 3.** DOS of the (5,5) SWCN (solid line) and (5,5) CNW (dash-dotted line).

with the bare SWCN, the low-frequency peaks in the CNW have a small upshift, while the high-frequency peaks are downshifted. This is due to the stiffening of the low-frequency modes in the former but the softening of the high-frequency modes in the latter. Moreover, there also appear some new peaks in the low-energy frequency region, resulted from the chain and tube interaction. The frequency shiftment and the new peaks in the low-frequency region may have an important influence on the low-temperature thermal properties.

As one of the fundamental thermal characteristic, specific heat  $C_V$  at temperature  $T$  is given by

$$C_V(T) = \int_0^{\omega_{\max}} k_B \left( \frac{\hbar\omega}{k_B T} \right)^2 \frac{\exp(\hbar\omega/k_B T)}{[\exp(\hbar\omega/k_B T) - 1]^2} g(\omega) d\omega, \quad (3)$$

with  $\hbar$  and  $k_B$  the Plank and Boltzmann constants, where  $g(\omega)$  is the vibrational DOS. Figure 4 shows the calculated specific heat of the (5,5) CNW and (5,5) SWCN. For both CNW and SWCN, the  $C_V$  increases with  $T$  increasing and would approach the classical value (not fully shown), independent of the particular systems.<sup>30</sup> This is because more and more phonon modes become populated with  $T$  increasing. At much low temperature, only the linearly acoustic phonons may contribute to  $C_V$ , and thus the  $C_V$  has a linear dependence on temperature,<sup>30</sup> as shown in Figure 4 inset by the dotted line. This indicates that a unique quantized phonon structures may be observed in the CNWs,<sup>31</sup> which may be universal in low-dimensional



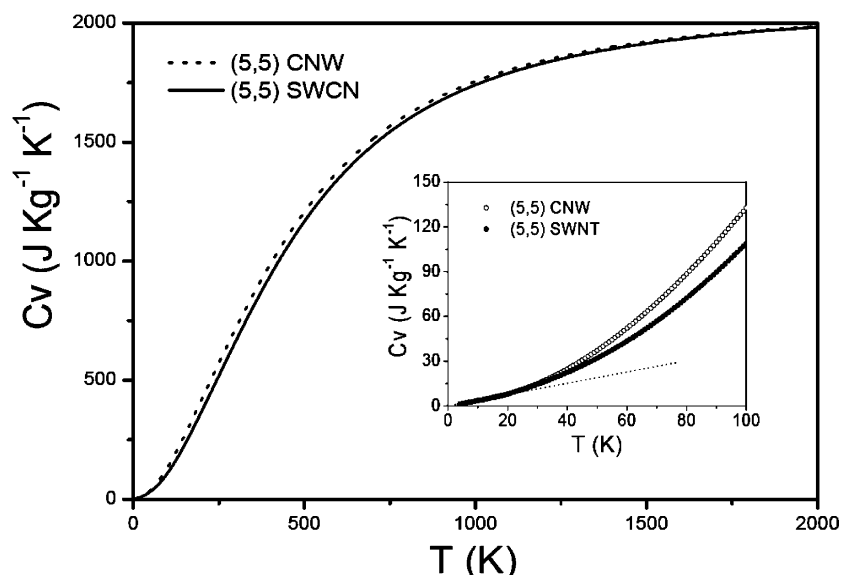


**Figure 4.** Specific heat of the (5,5) CNW (dashed line) and (5,5) SWCN (solid line). The inset is the blowup of  $C_V$  at low temperature, in which the open and solid circles correspond to the CNW and SWCN, respectively.

nanotube systems. In addition, the  $C_V$  in the former is larger than that in the latter, as shown in Figure 4. The larger  $C_V$  may indicate the larger thermal conductivity of the CNWs,<sup>32,33</sup> provided that the presence of carbon chain does not affect the phonon mean free path in nanotubes. Therefore, the CNWs may provide another candidate for thermal management in molecular electronics.<sup>34,35</sup>

## V. Summary

In summary, we investigate the phonon dispersion and specific heat of CNW with comparison of SWCN. Due to the van der Waals interaction between the carbon tube and chain, the twisting mode upshifts to a nonzero frequency of  $27\text{ cm}^{-1}$ , higher than the lowest optical phonon mode of a frequency  $9\text{ cm}^{-1}$ . It is found that the softening of G modes results mainly from the chain induced variations in the bond length on nanotube, independent of van der Waals interaction, while the stiffening of RBM are developed by the competition between the two factors. Interestingly, some new phonon modes are observed, come from the coupling vibrations of chain and tube. The bending and stretching modes of the chain are obtained to be about  $520\text{ cm}^{-1}$  and  $1935\text{ cm}^{-1}$  at  $\Gamma$  point, respectively. The frequency shiftment and some newly obtained vibrational modes can be observed by the Raman spectroscopy, which provide a simple and effective way in the characterization and thermal managements in the CNW-based molecular devices. Moreover, it is found that the vibration modes of CNWs depend strongly on the length of finite carbon chain, which would provide a way to identify the various lengths of chains confined in nanotube. From the chain length dependent vibration modes, it is expected that a finite chain of about 14 carbon atoms in the nanotube may produce the experimental Raman peak at about  $1850\text{ cm}^{-1}$ . In the low-frequency region, furthermore, the vibrational density of states are very different from that of the bare nanotube. The specific heat implies the underlying quantized phonon structures and much large thermal conductivity in the CNWs, which have the potential applications in the future CNW-based thermoelectrical devices.

**Acknowledgment.** This work was supported by National Natural Science Foundation of China (nos. 10674113 and

10374046), Hunan Provincial Natural Science Foundation of China (no. 04JJ3041), and partially by Scientific Research Fund of Hunan Provincial Education Department (no. 03B039).

## References and Notes

- (1) Blase, X.; Benedict, L. X.; Shirley, E. L.; Louie, S. G. *Phys. Rev. Lett.* **1994**, *72*, 1878.
- (2) Saito, R.; Dresselhaus, G.; Dresselhaus, M. S. *Physical Properties of Carbon Nanotubes*; Imperial College Press: London, 1998.
- (3) White, C. T.; Todorov, T. N. *Nature (London)* **1998**, *393*, 240.
- (4) Cao, J. X.; Yan, X. H.; Xiao, Y.; Tang, Y.; Ding, J. W. *Phys. Rev. B* **2003**, *67*, 045413.
- (5) Ding, J. W.; Yan, X. H.; Cao, J. X. *Phys. Rev. B* **2002**, *66*, 073401.
- (6) Schon, J. H.; Meng, H.; Bao, Z. N. *Science* **2001**, *294*, 2318.
- (7) H. W. Ch. Postma, Teepen, T.; Yao, Z.; Grifoni, M.; Dekker, C. *Science* **2001**, *293*, 76.
- (8) Pederson, M. R.; Broughton, J. Q. *Phys. Rev. Lett.* **1992**, *69*, 2689.
- (9) Miyamoto, Y.; Rubio, A.; Blase, X.; Cohen, M. L.; Louie, S. G. *Phys. Rev. Lett.* **1995**, *74*, 2993.
- (10) Okada, S.; Saito, S.; Oshiyama, A. *Phys. Rev. Lett.* **2001**, *86*, 3835.
- (11) Ajayan, P. M.; Iijima, S. *Nature (London)* **1993**, *361*, 333.
- (12) Smith, B. W.; Monthieux, M.; Luzzi, D. E. *Nature (London)* **1998**, *396*, 323.
- (13) Koga, K.; Gao, G. T.; Tanaka, H.; Zeng, X. C. *Nature (London)* **2001**, *412*, 802.
- (14) Lee, J.; Kim, H.; Kahng, S. J.; Kim, G.; Son, Y. -W.; Ihm, J.; Kato, H.; Wang, Z. W.; Okazaki, T.; Shinohara, H.; Kuk, Y. *Nature (London)* **2002**, *415*, 1005.
- (15) Wang, Z.; Ke, X.; Zhu, Z., et al. *Phys. Rev. B* **2000**, *61*, R2472.
- (16) Zhao, X.; Ando, Y.; Liu, Y.; Jinno, M.; Suzuki, T. *Phys. Rev. Lett.* **2003**, *90*, 187401.
- (17) McGuire, K.; Gothard, N.; Gai, P. L.; Dresselhaus, M. S.; Sumanasekera, G.; Rao, A. M. *Carbon* **2005**, *43*, 219.
- (18) Jinno, M.; Ando, Y.; Bandow, S.; Fan, J.; Yudasaka, M.; Iijima, S. *Chem. Phys. Lett.* **2006**, *418*, 109.
- (19) Fantini, C.; Cruz, E.; Jorio, A.; Terrones, M.; Terrones, H.; Van Lier, G.; Dresselhaus, M. S.; Saito, R.; Kim, Y. A.; Hayashi, T.; Muramatsu, H.; Endo, M.; Pimenta, M. A. *Phys. Rev. B* **2006**, *73*, 193408.
- (20) Liu, Y.; Jones, R. O.; Zhao, X. L.; Ando, Y. *Phys. Rev. B* **2003**, *68*, 125413.
- (21) Segall, M. D.; Lindan, P. L. D.; Probert, M. J.; Pickard, C. J.; Hasnip, P. J.; Clark, S. J.; Payne, M. C. *J. Phys.: Condens. Matter* **2002**, *14*, 2717.
- (22) Perdew, J. P.; Burke, K.; Ernzerhof, M. *Phys. Rev. Lett.* **1996**, *77*, 3865.
- (23) Vanderbilt, D. *Phys. Rev. B* **1990**, *41*, 7892.
- (24) Mao, Y. L.; Zhong, J. X.; Yuan, J. M.; Zhao, X. L.; Ando, Y. *J. Nanosci. Nanotechnol.* **2006**, *6*, 1482.
- (25) Rusznyak, A.; Zolyomi, V.; Kurti, J.; Yang, S.; Kertesz, M. *Phys. Rev. B* **2005**, *72*, 155420.

- (26) Xiao, Y.; Li, Z. M.; Yan, X. H.; Zhang, Y.; Mao, Y. L.; Yang, Y. R. *Phys. Rev. B* **2005**, *71*, 233405; Guo, Z. X.; Xiao, Y.; Ding, J. W.; Yan, X. H.; *Phys. Rev. B* **2006**, *73*, 045405.
- (27) Brenner, D. W. *Phys. Rev. B* **1990**, *42*, 9458.
- (28) Yamaguchi, Y.; Maruyama, S. *Chem. Phys. Lett.* **1998**, *286*, 336.
- (29) Yamaguchi, Y.; Gspann, J. *Phys. Rev. B* **2002**, *66*, 155408.
- (30) Popov, V. N. *Phys. Rev. B* **2002**, *66*, 153408.
- (31) Hone, J.; Batlogg, B.; Benes, Z.; Johnson, A. T.; Fischer, J. E. *Science* **2000**, *298*, 1730.
- (32) Hone, J.; Whitney, M.; Piskoti, C.; Zettl, A. *Phys. Rev. B* **1999**, *59*, R2514.
- (33) Xiao, Y.; Yan, X. H.; Cao, J. X.; Ding, J. W. *J. Phys.: Condens. Matter* **2003**, *15*, L341.
- (34) Lasjaunias, J. C.; Biljakovic, K.; Benes, Z.; Fischer, J. E.; Monceau, P. *Phys. Rev. B* **2002**, *65*, 113409.
- (35) Mizel, A.; Benedict, L. X.; Cohen, M. L.; Louie, S. G.; Zettl, A.; Budraa, N. K.; Beyermann, W. P. *Phys. Rev. B* **1999**, *60*, 3264.